

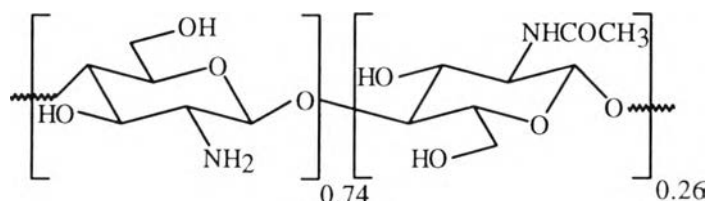
CHAPTER IV

RESULTS AND DISCUSSION

4.1 Determination of Degree of Deacetylation

Chitosan starting material with the degree of deacetylation of approximately 74.0% as determined by HPLC was used.

Scheme 4.1 Chemical structure of chitosan starting material



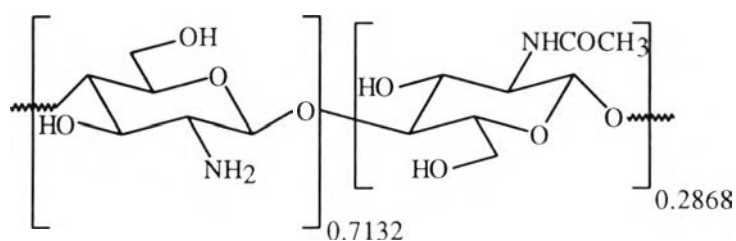
The elemental analysis (EA) of chitosan starting material shows the percent elements as follows.

Anal. Calcd. for $(C_6H_{11}O_4N)_{0.74} (C_8H_{13}O_5N)_{0.26}$: %C, 45.5095; %H, 6.7008; %O, 39.6463; %N, 8.1433. Found: %C, 39.32; %H, 7.15; %O, 46.23; %N, 7.30.

Generally, chitin-chitosan is a copolymer that cannot avoid the trace amount of mineral, especially $CaCO_3$, even from controlled extraction and purification process. Referred to specification of the starting material, the ash content of chitosan is approximately 0.2-0.6%. Thus, the EA results show the range differed from the calculated data.

Since chitosan did not perform the complete combustion, the result from EA did not show the exact %C. A compromised data evaluation can be done by using the N value as an internal standard according to the constant percent content from the chemical structure. As a result, C/N was used to evaluate %DD of chitosan starting material to be 71.32% (Scheme 4.2)

Figure 4.2 Real copolymer structure of chitosan starting material.



4.2 γ -Radiation Effects on Chitosan

In the present work, samples of chitosan (degree of deacetylation 71.32%) were irradiated with ⁶⁰Co γ -rays at various doses. After irradiation, an Ubbelohde viscometer was used on each sample in order to determine the intrinsic viscosity.

As shown in Figure 4.1, the intrinsic viscosity decreases significantly with an increasing in γ -ray amount up to 30 kGy and, decreases gradually after 30 kGy. Theoretically, the molecular weight will either increase by polymerization process or decrease by degradation process. In the present work, the decrease in intrinsic viscosity, or in another words, the molecular weight, was found. As a result, the system was evaluated to have chain degradation rather than chain combination.

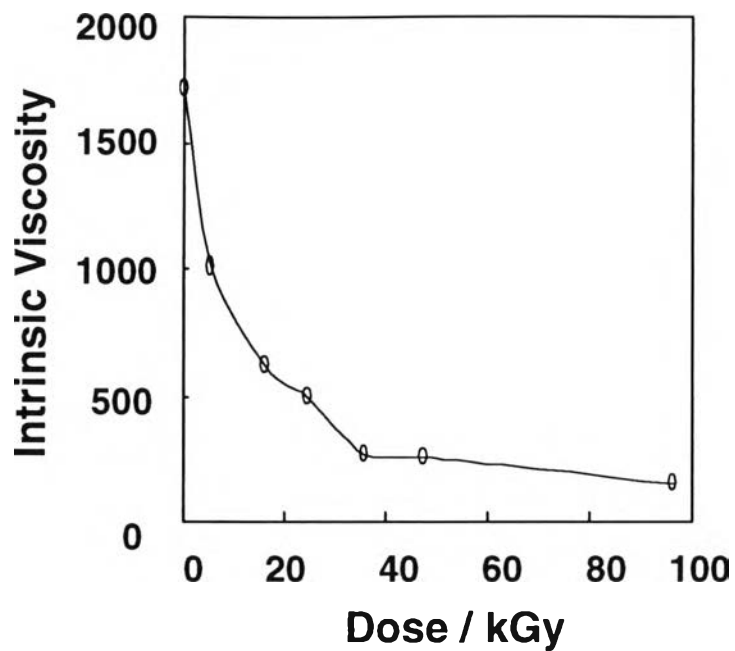


Figure 4.1 Intrinsic viscosity of chitosan irradiated in solid state as a function of γ -ray amount.

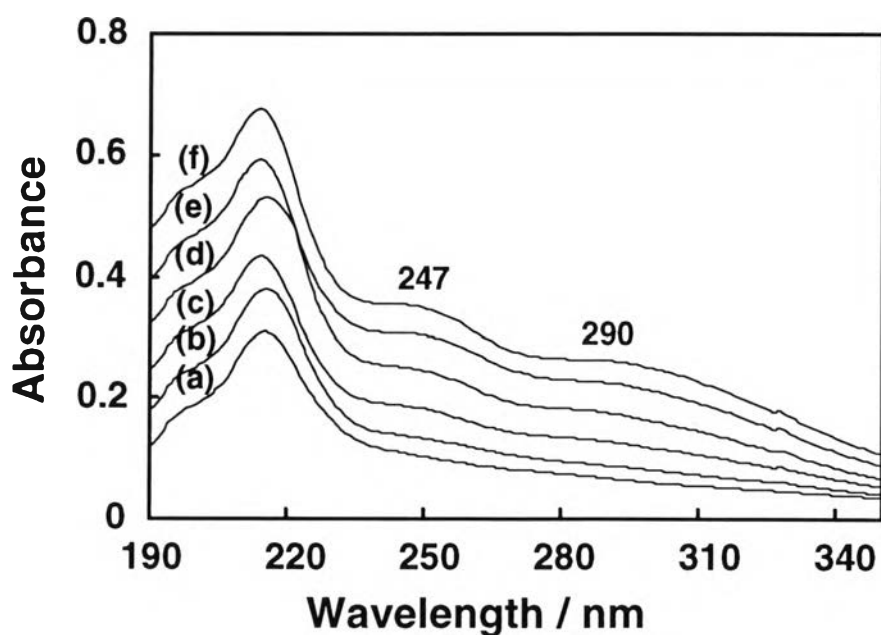
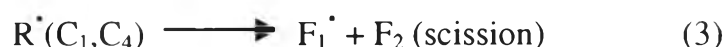
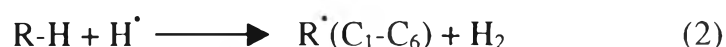
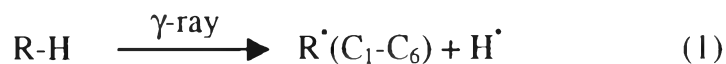


Figure 4.2 Absorption spectra of chitosan irradiated in solid state, (a) 0 kGy; (b) 5.51 kGy; (c) 16.08 kGy; (d) 24.53 kGy; (e) 35.96 kGy; and (f) 47.33 kGy. Measurements were done for 0.2 % chitosan solution in 0.04 M CH_3COOH .

Ershov *et al.* (1987) proposed the degradation mechanism for chitosan irradiated in solid state, as follow,



where R-H denotes chitosan macromolecule, R^\bullet is a chitosan macroradical localized on C_n carbon atom and F_1^\bullet , F_2 are fragments of main chain after scission.

According to the above mechanism (equation 1, 2, and 3), only a part of chitosan macroradicals localized on C_1 and C_4 carbon atoms undergo transformation with scission of 1-4 glycosidic bond, that is equivalent to main chain scission.

After chitosan was irradiated, the obtained product was dissolved in 0.04M CH_3COOH in order to study the structural changing by UV spectroscopy. As shown in Figure 4.2, chitosan solution shows 2 peaks at 247, and 290 nm referred to carbonyl, and carboxyl groups, respectively.

In order to study the total amount of carbonyl and carboxyl group changing, UV absorbance at 247 and 290 nm were plotted with the amount of γ -ray. Figure 4.3 shows that when the amount of γ -ray is increased, the absorbance at 247 and 290 is also increased significantly. This implies that the structure of γ -irradiated chitosan was changed to the structure with carbonyl and carboxyl group.

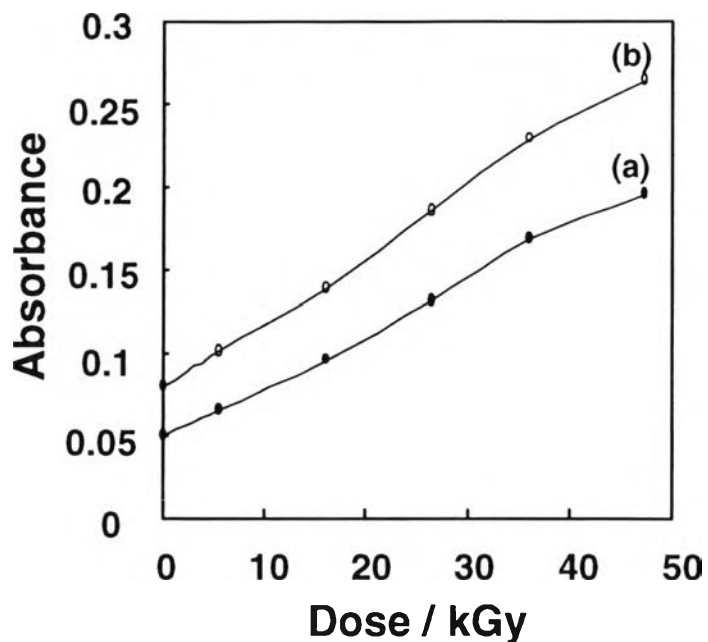


Figure 4.3 Increase in the amount of; (a) carboxyl groups, and (b) carbonyl groups, as a function of absorbed dose.

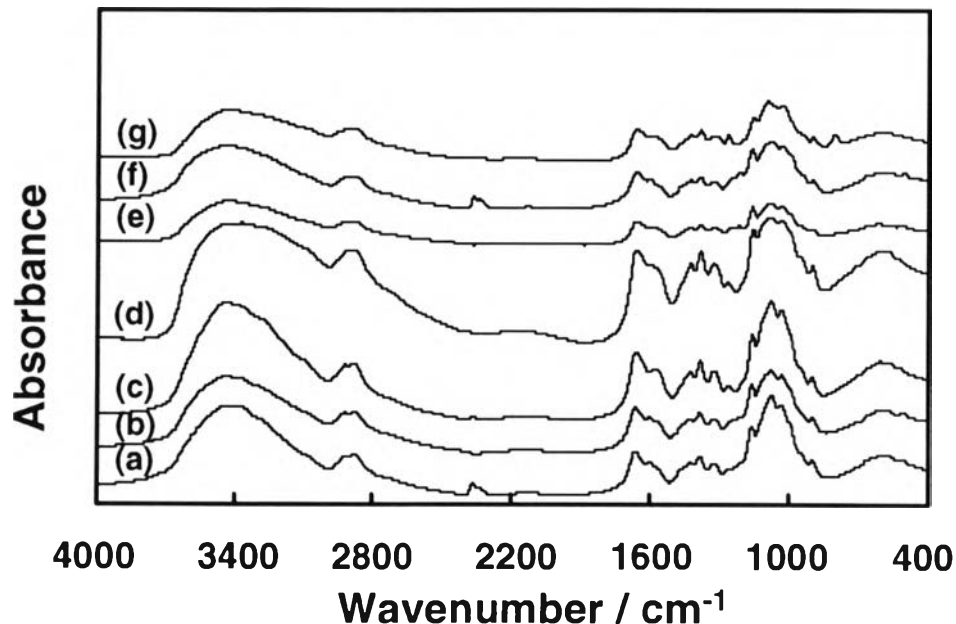
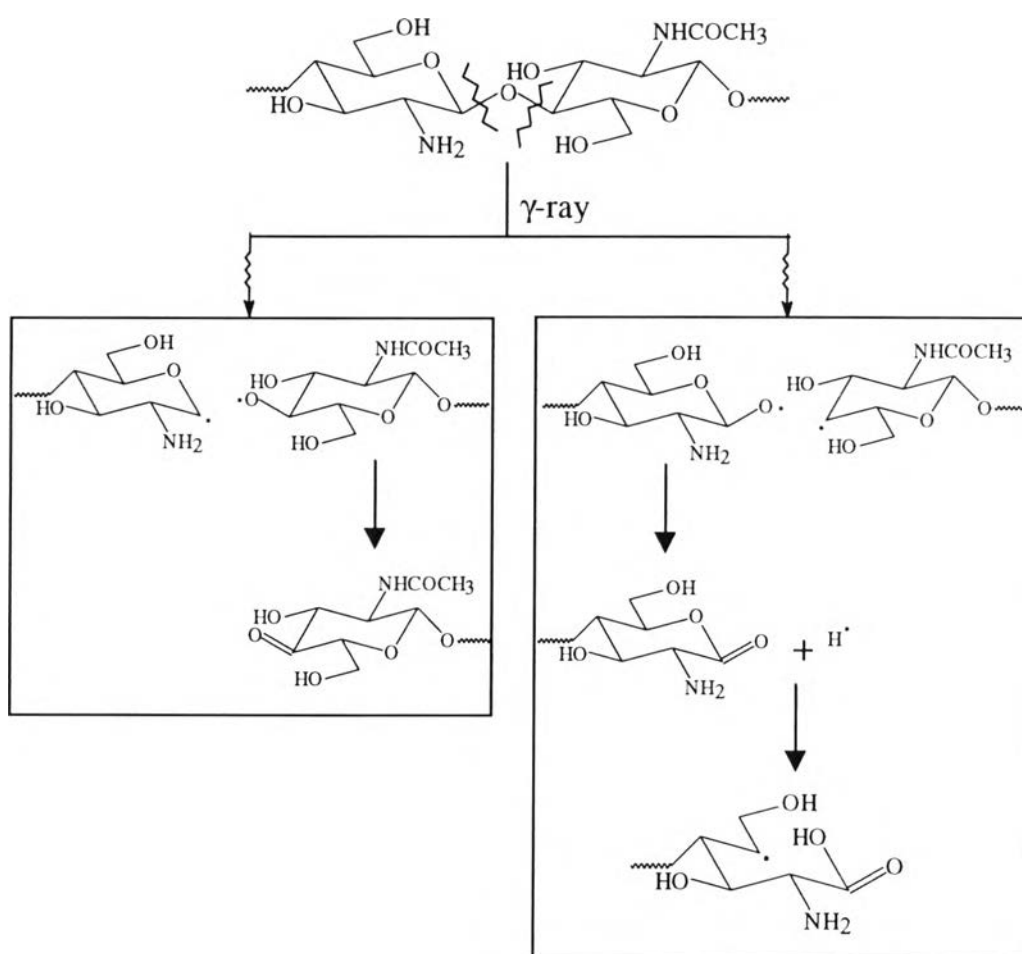


Figure 4.4 FT-IR spectra of chitosan irradiated in solid state, (a) 0 kGy; (b) 5.51 kGy; (c) 16.08 kGy; (d) 26.43 kGy; (e) 35.96 kGy; (f) 47.33 kGy; and (g) 96.23 kGy.

FT-IR (KBr, cm^{-1}): 3439 (O-H), 2879 (C-H), 1656 (C=O amide), and 895 (pyranose ring).

The possibilities of these structures reported by Ulanski *et al.* (1992) are shown in Scheme 4.3.

Scheme 4.3 Mechanism of carbonyl and carboxyl formation
(Ulanski *et al.*, 1992)



Thus, after γ -irradiation, the radicals were formed in the chitosan chain. The decomposition of these radicals, then, caused the formation of carbonyl and carboxyl groups.

Figure 4.4 shows the chemical structure of chitosan irradiated in solid state observed by FT-IR technique. The characteristic peak at 895 cm^{-1} , which belongs to pyranose rings, still remained in the structure. This implied that the γ -ray up to 96.23 kGy does not destroy the chemical structure of chitosan.

Since the biocompatibility is not affected by an irradiation dose of 25 kGy (Ulanski *et. al.*, 1992) and the degree of deacetylation dose not change (Lim *et. al.*, 1998) at this dose, the optimum dose for chitosan chain degradation in the present work is considered around 25 kGy.

4.3 Preparation of N-Phthaloyl Oligochitosan

Protection by phthalimido groups was chosen as the most suitable protection for the amino groups of chitosan. This protection will allow the further reaction occurring selectively at the primary hydroxyl group of C-6 position and/or secondary hydroxyl group at C-3 position. The use of phthaloyl protection of the primary amino groups of chitosan gave a derivative having a much improved solubility in organic solvents such as DMF, DMAc, DMSO, and pyridine. High solubility of N-phthaloyl chitosan has enabled various modification reactions to proceed quantitatively in homogeneous system. As suggested by the solubility of N-phthaloylated chitin in DMSO (Kurita *et al.*, 1982) the phthaloyl group is effective to impart solubility owing to the bulky nature and completed removal of N-attached hydrogens that form intermolecular hydrogen bonds. The preparative procedures based on N-phthaloyl chitosan are useful for regioselective and quantitative introduction of substituents. After desired modification reactions, the phthaloyl groups are easily removed with hydrazine to regenerate the free amino groups.

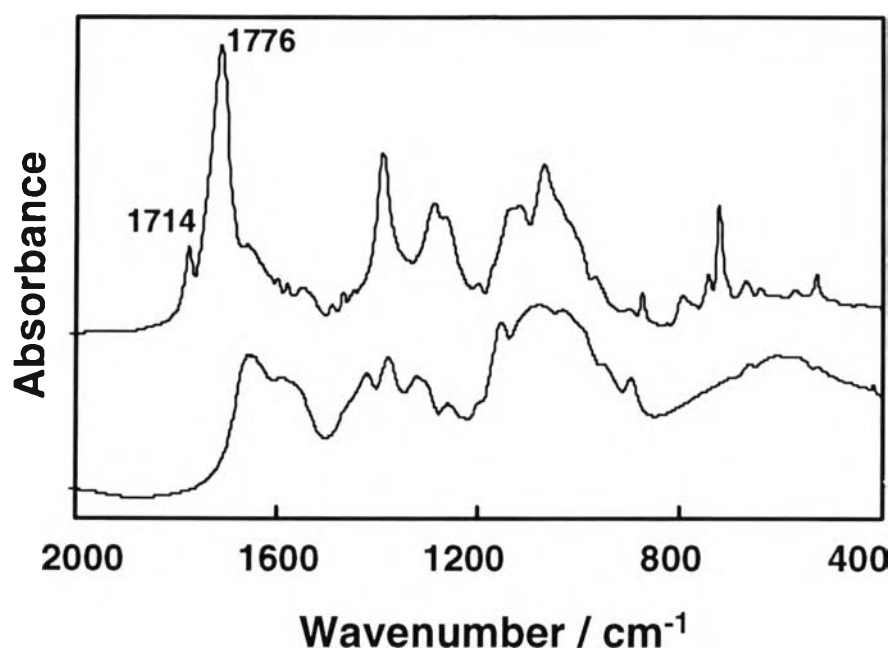


Figure 4.5 FT-IR spectra of (a) chitosan (DD = 71.32%), and (b) N-phthaloyl oligochitosan.

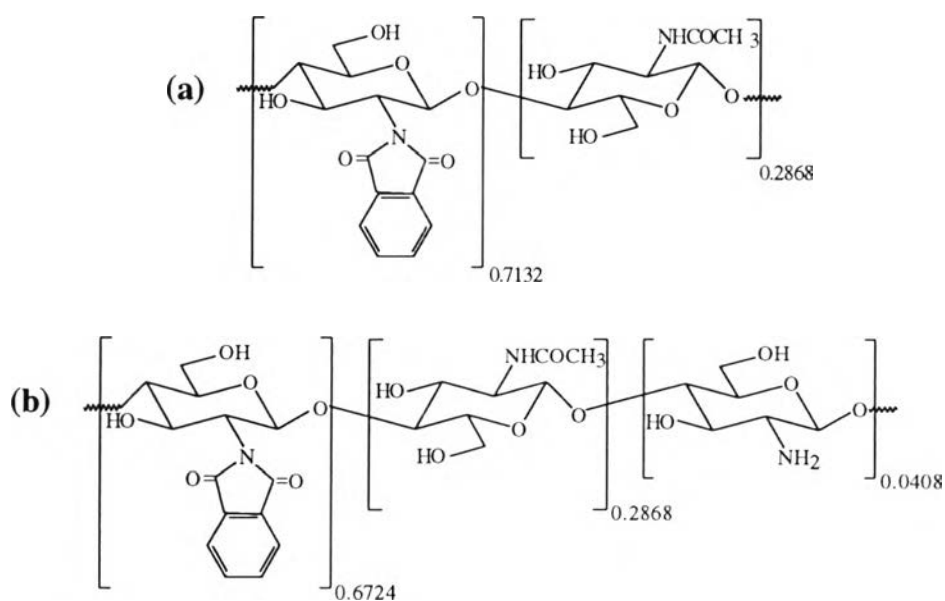
FT-IR (KBr, cm⁻¹): 3439 (O-H), 2879 (C-H), 1714, and 1776 (C=O of phthalimido group, 1656 (C=O amide), and 895 (pyranose ring).

The characteristic absorptions due to phthalimido groups at 1714 and 1776 cm^{-1} were observed in the FT-IR spectrum as shown in Figure 4.5.

$^1\text{H-NMR}$ and $^{13}\text{C-NMR}$ were also applied to characterize the modified structure. In Figure 4.6, the proton peaks can be referred to acetyl methyls at 1.8 ppm, pyranose rings at around 3-5.5 ppm, and benzene rings in phthalimido groups at around 7-8 ppm. Figure 4.7 shows carbon peaks due to acetyl methyls, pyranose rings, aromatic rings, and carbonyl at 20, 55-110, 122-140, and 168 ppm, respectively. Hence, the NMR result implied the successful of N-phthaloylation.

The elemental analysis (EA) of N-phthaloyl oligochitosan shows the percent elements as follows. Anal. Calcd. for $(\text{C}_{14}\text{H}_{13}\text{O}_6\text{N})_{0.7132} (\text{C}_8\text{H}_{13}\text{O}_5\text{N})_{0.2868}$: %C, 55.4447; %H, 4.8916; %O, 34.3960; %N, 5.2679. Found: %C, 55.1275; %H, 4.445; %O, 37.0775; %N, 3.35.

Scheme 4.4 Structure of N-phthaloyl oligochitosan obtained from chitosan with %DD = 71.32. (a) ideal structure with completion of phthalimido group, and (b) 97.34% phthalimido group induced structure.



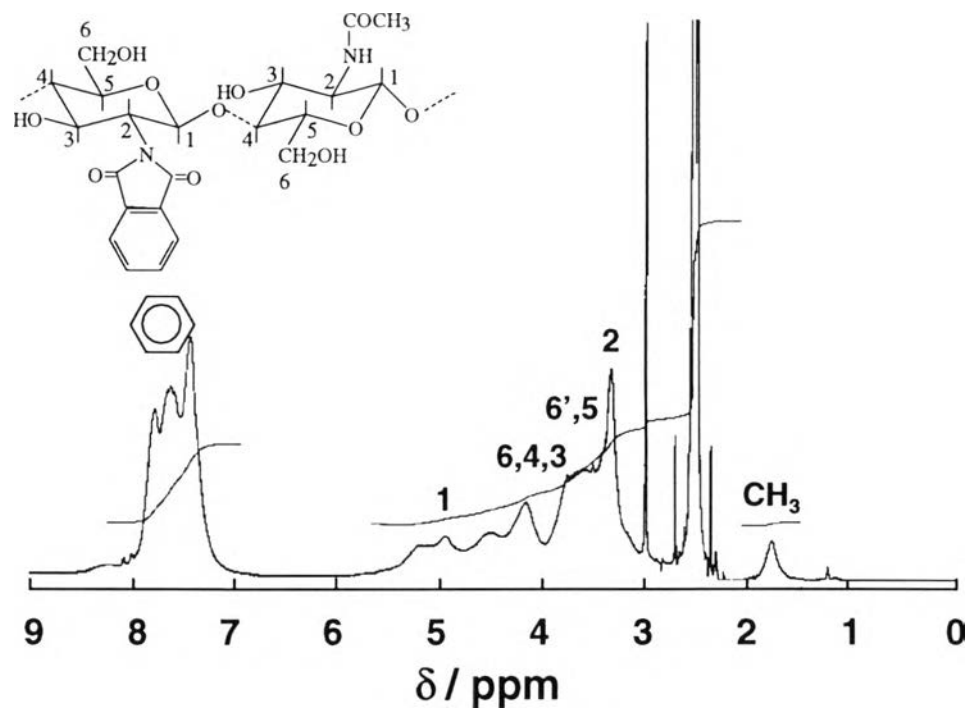


Figure 4.6 400 MHz ¹H-NMR spectrum of N-phthaloyl oligochitosan, in DMSO-d₆, at 25°C.

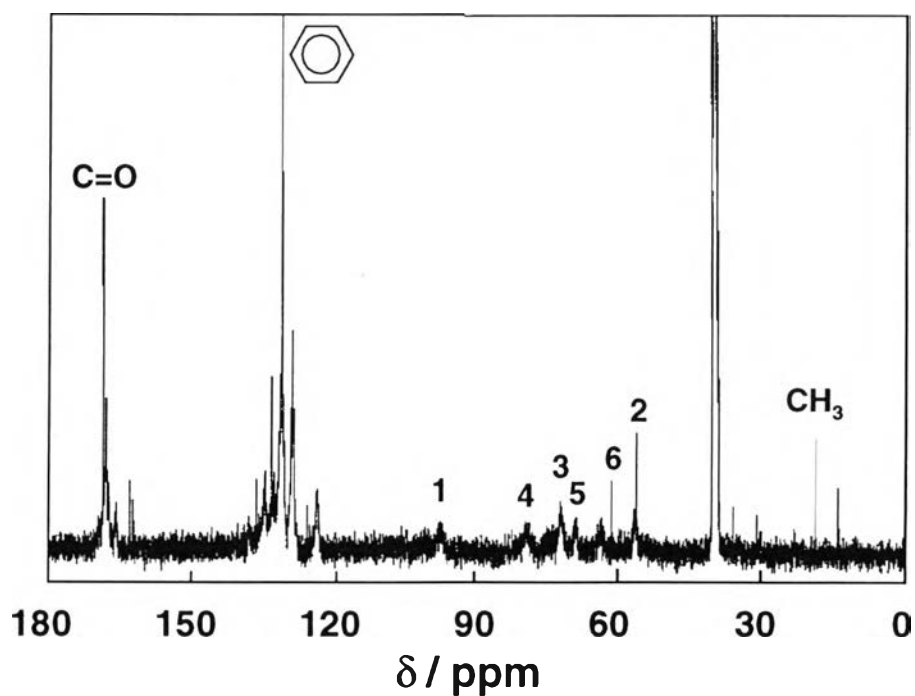


Figure 4.7 400 MHz ¹³C-NMR spectrum of N-phthaloyl oligochitosan, in DMSO-d₆, at 25°C.

The analytical data suggested that the reactivity of N-phthaloylation was 97.34%. Thus, the structure of N-phthaloyl oligochitosan in this present work is shown in Scheme 4.4.

In Figure 4.8, Phthalimido chromophore shows λ_{\max} at 238 nm. The λ_{\max} of N-phthaloyl oligochitosan was corresponded to that of phthalimido chromophore. This means that some phthalimido groups were released out from oligochitosan chain in basic condition. In another word, the preparation of N-phthaloyl oligochitosan was successful.

Thermal stability of chitosan starting material is shown in Figure 4.9. TGA shows the weight loss at 58.42°C followed by the second peak at 320.04°C, which can also be seen as two endothermic peaks in DTA. The former decay reveals the loss of moisture and water content in chitosan starting material. The latter peak shows the degradation of chitosan, which might be owing to the breakage of glucosidic bond between pyranose rings.

Figure 4.10 shows three endothermic peaks of DTA, which corresponds to the weight loss in TGA. TGA reveals that there is the moisture absorbed in the derivatives as confirmed from the weight loss at 53.43°C while the degradation of phthalimido groups shows weight loss at 220.74°C, as referred to the observation in Figure 4.9. The last peak at 390.93°C revealed the bond breaking of glucoside linkage. The result implied that the introduction of phthalimido groups onto chitosan influence to the thermal stability.

Figure 4.11 shows the XRD patterns of oligochitosan at 9.82° as well as 19.88° and N-phthaloyl oligochitosan at 19.08°. It was found that the peak was broader after N-phthaloylation. This implied the decreasing of the crystalline, which might be due to the introduction of bulky phthalimido groups. As a result, the loose of chitosan chain packing was formed.

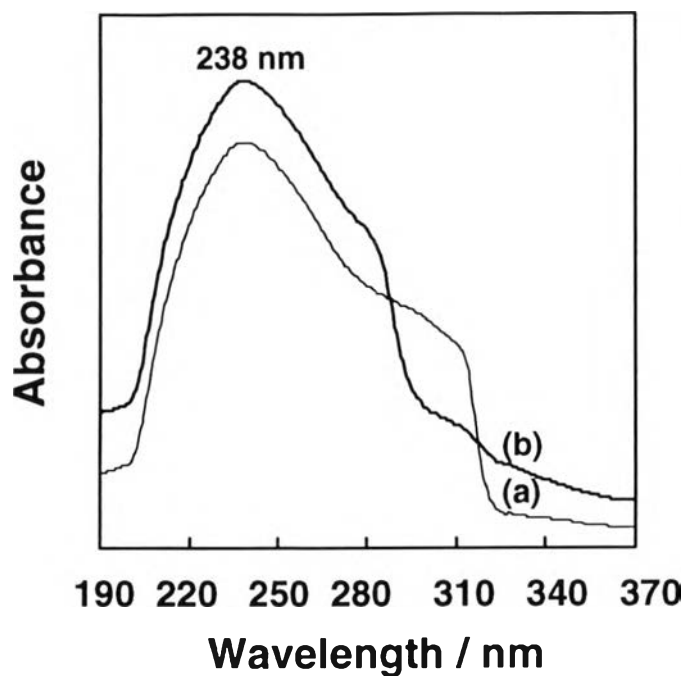


Figure 4.8 Absorption spectra of (a) phthalic anhydride, and (b) N-phthaloyl oligochitosan in 0.5 M NaOH.

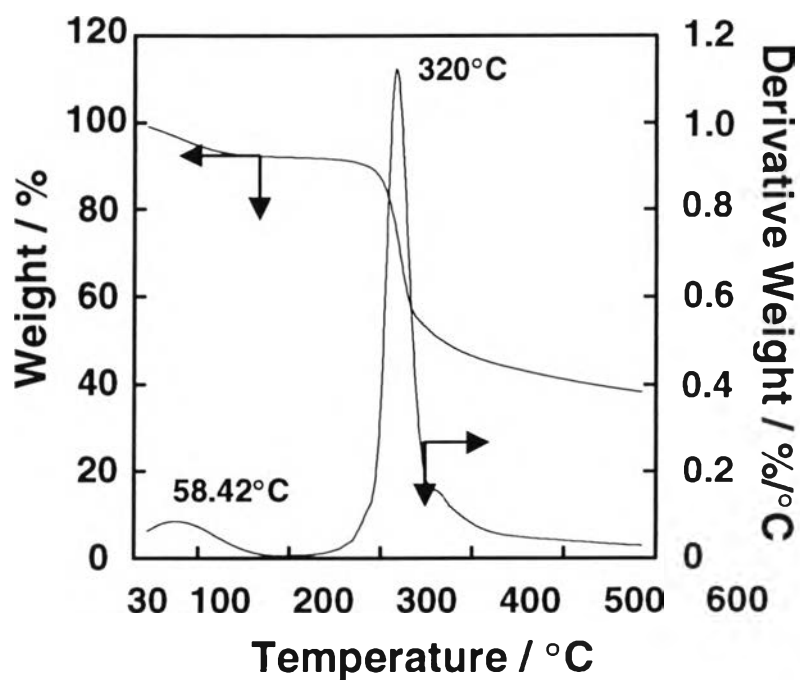


Figure 4.9 TGA and DTA diagrams of irradiated chitosan with dose 26.43 kGy.

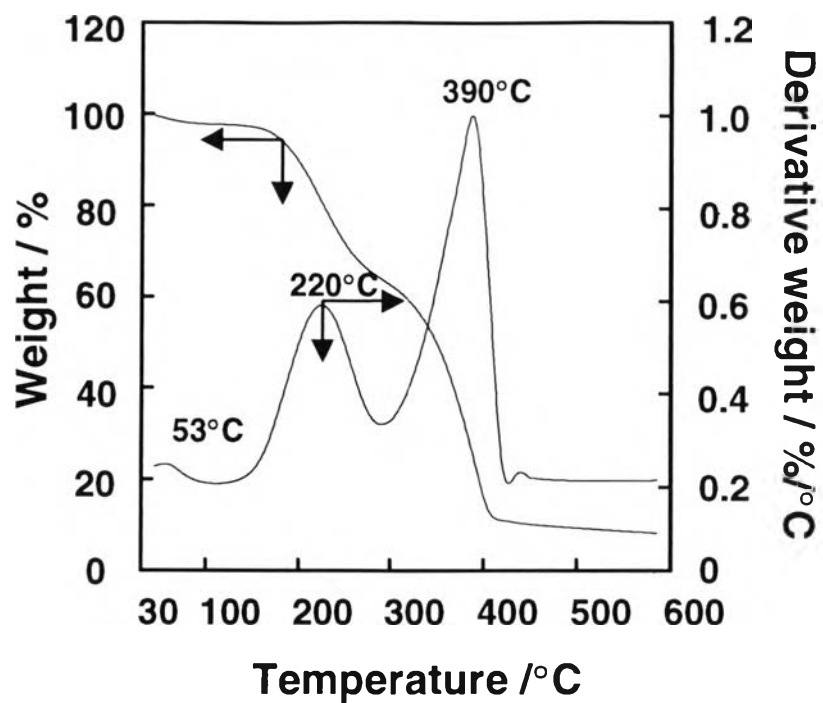


Figure 4.10 TGA and DTA diagrams of N-phthaloyl oligochitosan.

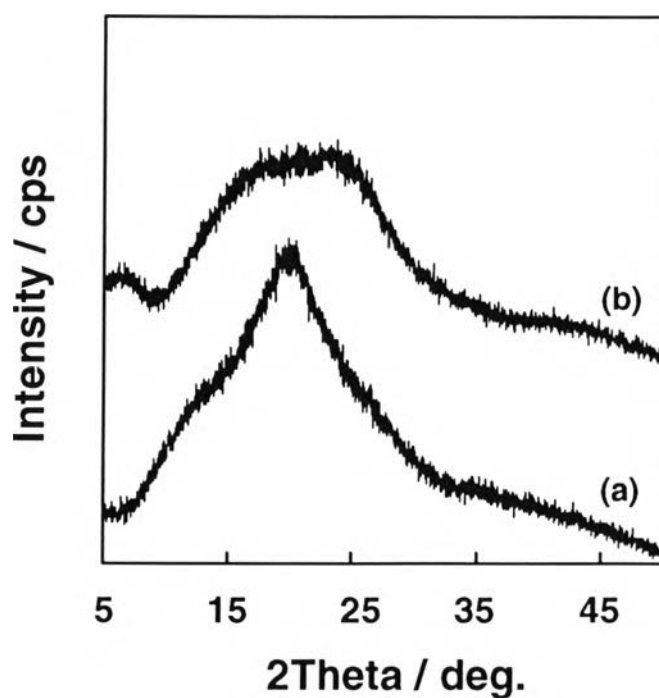


Figure 4.11 XRD patterns of (a) oligochitosan (DD=71.32%), (b) N-phthaloyl oligochitosan.

4.4 Preparation of Chitosan Precursors

The chemical modification of γ -irradiated chitosan was studied in order to obtain the reactive derivatives. There are two different reactive functional groups, i.e., the hydroxyl and the amino groups on chitosan main chain, which can be experienced to chemical reaction.

The present work is focused on two different types of modification at C-6 position, i.e., the reactive ester by coupling agent and oxidation.

4.4.1 Synthesis of N-Phthaloyl Oligochitosan-Carbonyl Imidazolide

The use of coupling agent is one of the interesting approaches for polymer-drug conjugation. In this case, the spacer formed by the coupling agent is a key factor to achieve controlled release system. In the present work, *N,N'*-carbonyl diimidazole (CDI) was chosen as a coupling agent to form an activated ester owing to its high reactivity with alcohols, carboxylic acids, amines, etc.

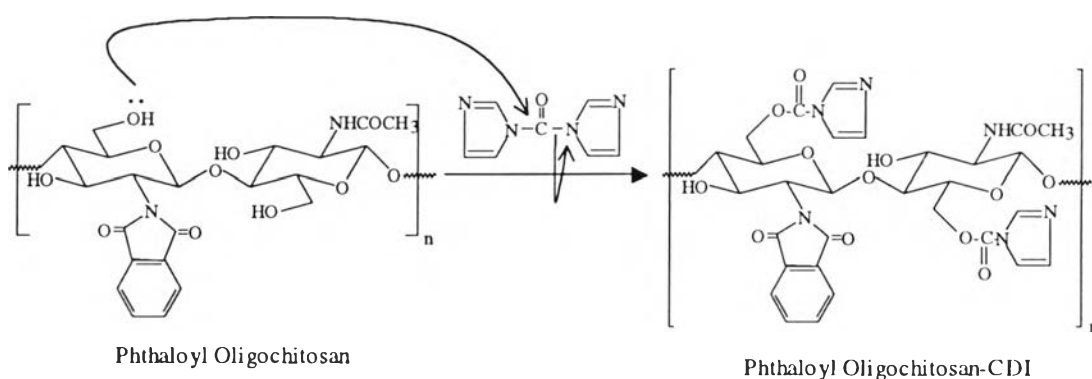
Simionescu *et al.* (1985) reported that dicyclohexylcarbodiimide (DCC) is an effective coupling agent for the introduction of chloramphenicol into Biozan R[®] to apply as a drug delivery system. This study showed that introducing spacer would improve for not only the stabilization but also the solubility. *N,N'*-carbonyldiimidaazole (CDI) was reported to be a spacer for the controlled release of chitosan conjugated chloramphenicol (Chunharotrit *et al.*, 1998) and carbaryl (Lertworasirikul *et al.*, 1999) by reactive ester formation. Generally, the reaction with *N,N'*-carbonyl diimidazole is progressed by the nucleophilic substitution mechanism in which both hydroxyl and amino can act as a nucleophile. To avoid a complicated work, the amino groups at C-2 position of chitosan are protected in order to achieve chemically modified at only C-6 position.

According to the high reactivity of CDI with water, the reaction condition should be concerned on non-aqueous system in order to avoid the CDI degradation. *N,N*-dimethylformamide (DMF), and *N,N*-dimethylacetamide (DMAc) are considered to be a suitable solvent for this reaction. Owing to the high solubility of *N*-phthaloyl oligochitosan in these organic solvents, the reaction can be operated under homogeneous condition.

The FT-IR spectrum is shown in Figure 4.12. The obtained product showed the absorbance at 1774 cm^{-1} , which is the characteristic peak of an activated ester carbonyl of imidazolide. The pyranose ring shows characteristic peak at 905 cm^{-1} suggesting that the saccharide unit is not degraded by the reaction.

The mechanism of the active ester formation is shown in Scheme 4.5. Owing to a very high reactivity toward nucleophilic reagent of CDI, the electron attraction exerts from both sides on the carbonyl group by the heterocyclic ring.

Scheme 4.5 Reaction mechanism of *N*-phthaloyl oligochitosan with CDI



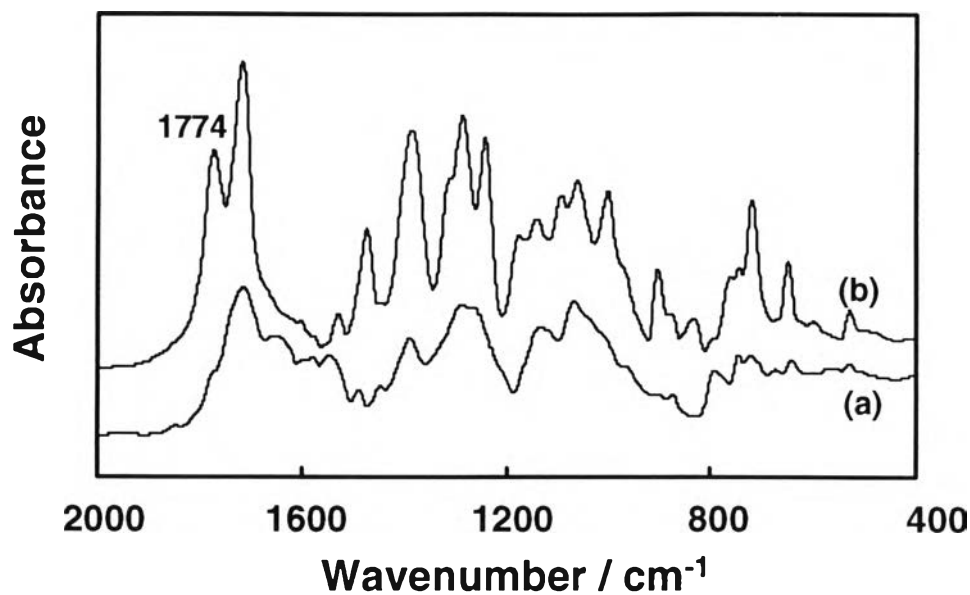


Figure 4.12 FT-IR spectra of (a) N-phthaloyl oligochitosan, and (b) N-phthaloyl oligochitosan-CDI.

FT-IR (KBr, cm^{-1}): 1658 (C=O amide), 1771 (-COO-imidazolidine), 1715, and 1776 (C=O of phthalimido group), 905 (pyranose rings).

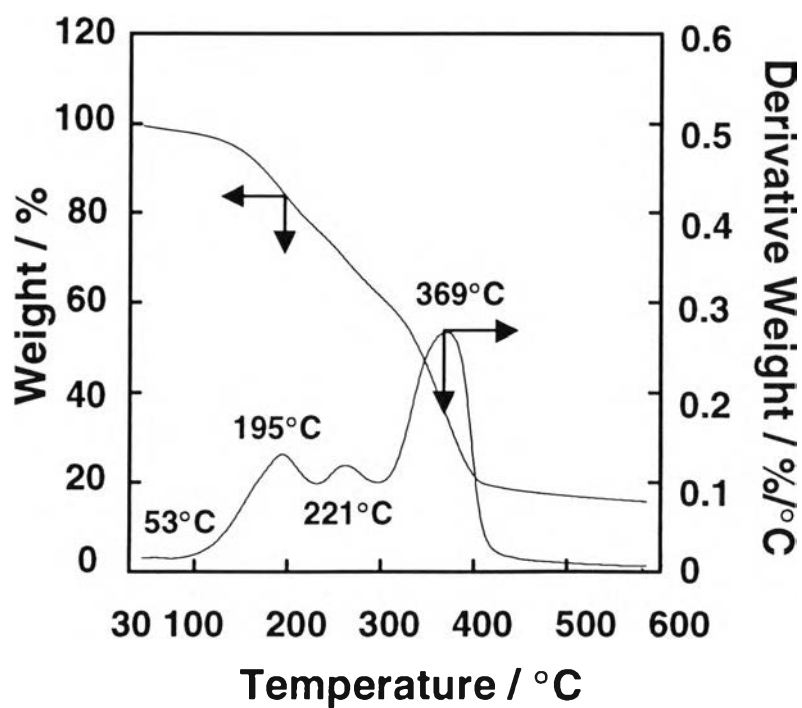


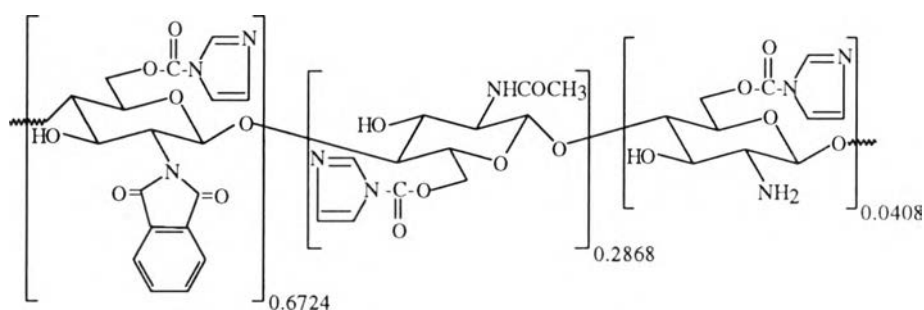
Figure 4.13 TGA and DTA diagrams of N-phthaloyl oligochitosan-CDI.

In this reaction, by-products obtained were an imidazole. The purification process was necessary by thoroughly washing the obtained product with methanol several times to eliminate imidazole and remove the excess CDI.

The elemental analysis (EA) result is shown below: Anal. Calcd. for $(C_{18}H_{16}O_7N)_0.6724 (C_{13}H_{15}O_6N_5)_0.0408 (C_{12}H_{15}O_6N_3)_0.2868$: %C, 53.8119; %H, 4.3720; %O, 29.7968; %N, 12.0350. Found: %C, 54.1410; %H, 4.5510; %O, 30.6534; %N, 10.6625.

The calculation from ideal structure (Scheme 4.6) gave the nitrogen content equal to 12.04% while the found value showed only 9.445%. The result implied that carbonyldiimidazole (CDI) was introduced for 78.48%.

Scheme 4.6 Ideal structure of N-phthaloyl oligochitosan-carbonyl imidazolid.



After the reaction, TGA and DTA diagram of the compound shows four endothermic peaks (Figure 4.13). The weight loss at the initial step refers to the loss of moisture and water. Comparing to that of N-phthaloyl oligochitosan (Figure 4.10) the peak at around 194.75°C reveals the loss of phthalimido groups and the peak at 261.09°C reflects the loss of imidazolid. The peak at 369.27°C is due to the breaking of the glucoside linkage. This implies the successful introduction of CDI onto N-phthaloyl oligochitosan chain.

It is known that when chitosan was modified, the packing characteristic of chitosan will be different from the original one. X-ray analysis is an alternative way to observe the changing. The XRD pattern of N-phthaloyl oligochitosan shows 2θ at 19.08° while N-phthaloyl oligochitosan-CDI shows at 22.66° (Figure 4.14). The peak of the N-phthaloyl oligochitosan-CDI became more significant. This implies that, although the bulky groups of activate ester was introduced into the chain, the chain packing was more preferable, which might be due to the intramolecular chain interaction of the ester group, such as the strong H-bonding between ester oxygen and hydroxyl group of chitosan.

4.4.2 Synthesis of Carboxyl N-Phthaloyl Oligochitosan

Oxidation of chitin-chitosan is interesting as a mean of introduction of new functional groups into the polymer chain. It can be expected to obtain a reactive precursor for further reaction with a model drug having alcohol or amine moiety to form an ester or amide compound. Another advantage also can be mentioned as an introduction of the spacer, such as, acid chloride to get more reactive chitosan.

Here, chromium trioxide in acetic acid was applied as a chromic acid oxidant.

The characterization by FT-IR could not be done successfully since the changing of functional group in oxidation is very small. Figure 4.15 shows the broad peak around 3500 cm^{-1} , implied the intramolecular hydrogen bonding enhanced after oxidation. The absorbance of C=O in carboxylic acid occurs near C=O of phthalimido group in N-phthaloyl oligochitosan which makes it difficult to clarify from this peak. However, It should be noted that the obtained product was a blue color powder. This implies that some chromium ions from the oxidant were still entrapped in the chitosan structure owing to the ion interaction property of chitosan itself.

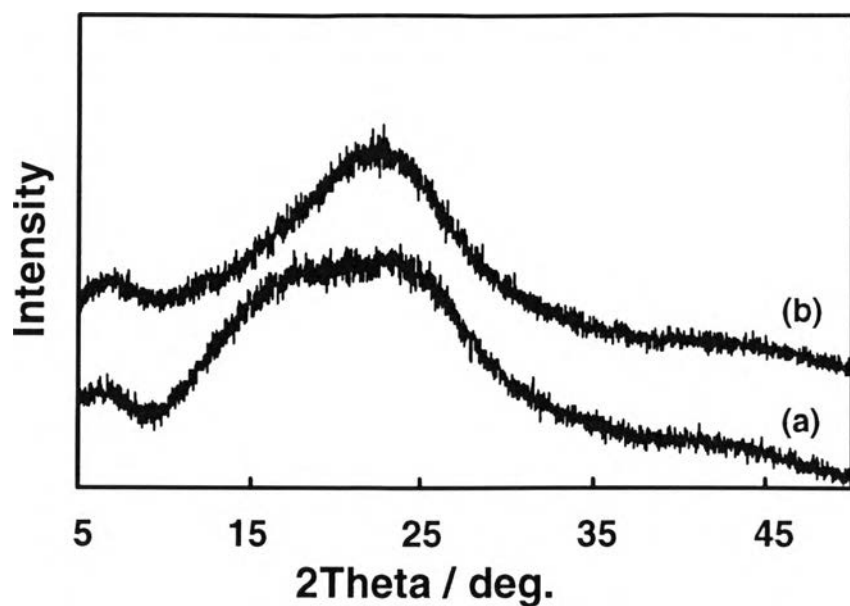


Figure 4.14 XRD patterns of (a) N-phthaloyl oligochitosan, and (b) N-phthaloyl oligochitosan-CDI.

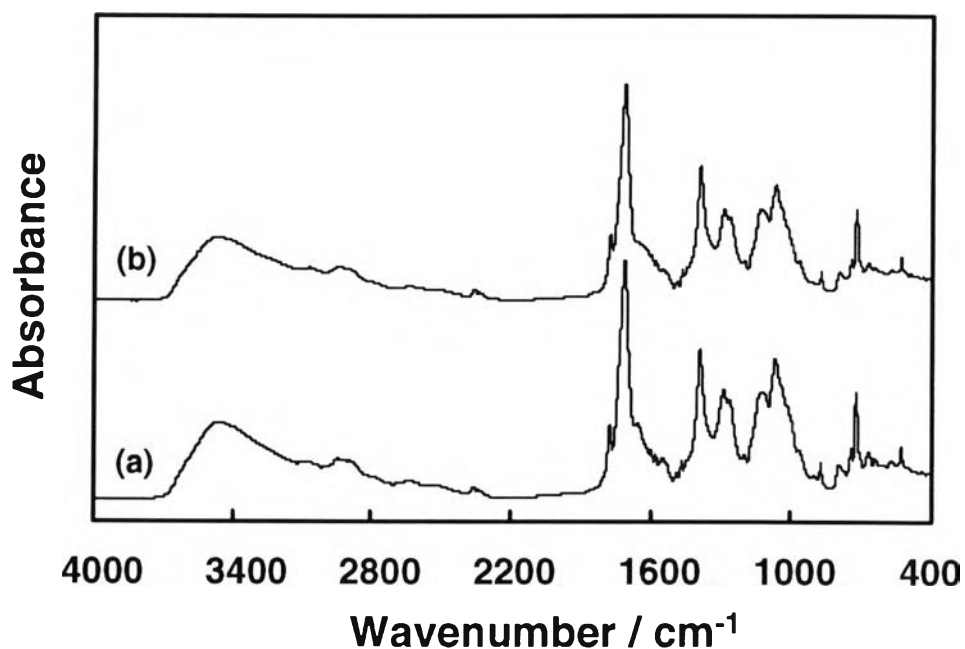


Figure 4.15 FT-IR spectra of (a) N-phthaloyl oligochitosan, and (b) carboxyl N-phthaloyl oligochitosan.

FT-IR (KBr, cm⁻¹): 3469 (OH stretching), 1714 (C=O acid) 1715 and 1776 (C=O amide), 875 (pyranose rings).

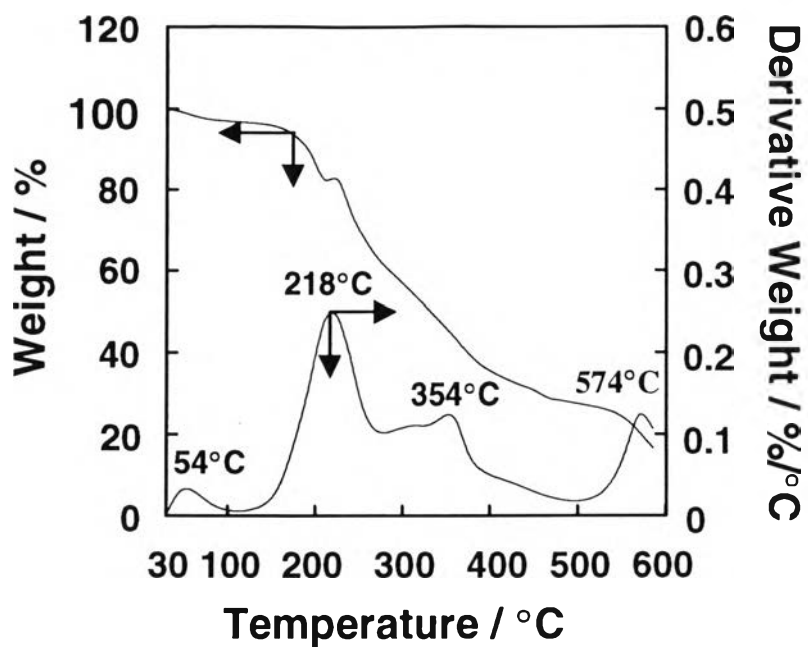


Figure 4.16 TGA and DTA diagrams of carboxyl N-phthaloyl oligochitosan.

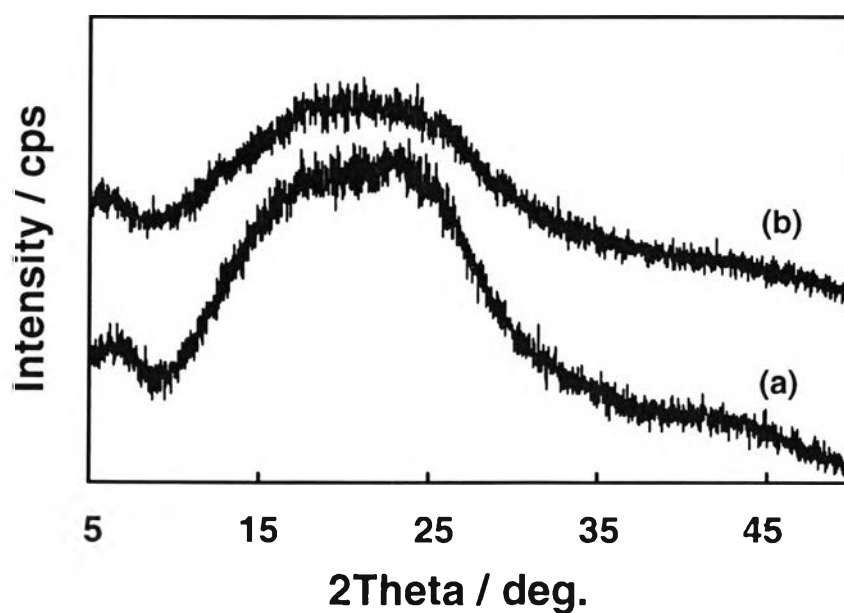


Figure 4.17 XRD patterns of (a) N-phthaloyl oligochitosan, and (b) carboxyl N-phthaloyl oligochitosan.

In this present work, the obtained product was further purified by thoroughly washing with diluted hydrochloric acid several times to eliminate chromium ion and then methanol to remove the excess oxidant. However, the complete decolorization could not be achieved. It is known that amino group of chitosan can act as a chelating group for various metal ions; thus, the blue colorizing may be due to the complexation of chromium and some part of chitosan chain.

The successful of the synthesis can be claimed to the solubility improvement in solvent, even in water at room temperature (Horton *et al.*, 1973).

Figure 4.16 shows thermal stability of carboxyl N-phthaloyl oligochitosan. Phthalimido group shows weight loss at 218.62°C. Whereas, pyranose ring degradation was observed at 354.20°C. The last peak at 574.87°C may be due to some salt formation of some chromium, which entrapped in the amino unit.

Figure 4.17 shows the packing structure of carboxyl N-phthaloyl oligochitosan compared with N-phthaloyl oligochitosan. XRD pattern of N-phthaloyl oligochitosan shows 2θ at 19.08° and at 19.66° of carboxyl N-phthaloyl oligochitosan.

It should be noted that carboxyl N-phthaloyl oligochitosan is an effective method since the reaction is not required the expensive reagent. Though it shows the problem of chromium ion entrapped, it is the only product that is easy to be dissolved in various solvents, and water. However, this method still has the problem on the complex formation between metal oxidant and chitosan. The elimination of chromium ion from the product is a problem to be studied and solved in the future.